Gen Relativ Gravit (2013) 45:2053–2073
DOI 10.1007/s10714-013-1578-x

RESEARCH ARTICLE

Cold, ultracold and Nariai black holes with quintessence

Sharmanthie Fernando

Received: 13 March 2013 / Accepted: 30 July 2013 / Published online: 8 August 2013

Abstract In this paper, we study the properties of the charged black hole surrounded by the quintessence. The solution space for the horizons for various values of the mass M, charge Q, and the quintessence parameter α are studied in detail. Special focus in given to the degenerate horizons: we obtain cold, ultracold and Nariai black holes which has similar topologies as for the Reissner–Nordstrom-de Sitter black holes. We also study the lukewarm black hole with the quintessence in this paper.

Keywords Static · Charged · Quintessence · Nariai · Cold · Ultra-cold · Lukewarm

1 Introduction

There are strong observational support for the fact that universe is undergoing accelerated expansion leading to the presence of dark energy [1–3]. It is one of the greatest challenges in modern physics to seek solutions as to why and how this acceleration occurs. Various dynamical models of dark energy have been considered in the literature to explain the acceleration [4]. Most of these models involve a dynamical scalar field. In this paper, we investigate black holes surrounded by quintessence matter. Quintessence field is a scalar field coupled to gravity and is a candidate for dark energy. There are many works that have focused on the quintessence model. An extended quintessence model has been proposed by coupling the scalar field to the Ricci scalar in [5]. The correspondence between the quintessence and the tachyon dark energy has been studied in [6]. Dynamics of the phantom energy interacting with quintessence models are presented in [7]. Local measurements that can detect the quintessence field has

S. Fernando (✉)
Department of Physics and Geology, Northern Kentucky University,
Highland Heights, KY41099, USA
e-mail: fernando@nku.edu

been suggested in [8]. Kiselev [9] derived black hole solutions surrounded by the quintessence matter in an interesting paper. In this paper, we will focus on studying the properties of charged black holes surrounded by the quintessence.

The paper is organized as follows. In Sect. 2 we introduce the charged black hole surrounded by the quintessence. In Sect. 3, we discuss the free quintessence model. In Sect. 4, the Reissnner–Nordstrom black hole with and without the cosmological constant is compared with the charged black hole with the quintessence. In Sect. 5 and 6, the solution space of the horizons are discussed. In Sect. 7, the charged Nariai and the cold black holes are discussed. In Sect. 8, the ultra-cold black hole is presented. In Sect. 9, the lukewarm black hole is given. Finally, in Sect. 10, the conclusions are given.

2 Charged black hole surrounded by the quintessence

In this section, we will give an introduction to the charged black hole surrounded by the quintessence, which was derived by Kiselev [9]. The geometry of the black hole is given by the metric,

$$ds^2 = -f(r)dt^2 + \frac{dr^2}{f(r)} + r^2(d\theta^2 + sin^2\theta d\phi^2) \tag{1}$$

Here,

$$f(r) = 1 - \frac{2M}{r} + \frac{Q^2}{r^2} - \frac{\alpha}{r^{3w_q+1}} \tag{2}$$

and M is the mass, Q is the charge, α a normalization factor and w_q is the state parameter of the quintessence matter. In this paper, the parameter w_q has the range,

$$-1 < w_q < -\frac{1}{3} \tag{3}$$

The quintessence matter has the equation of state as,

$$p_q = w_q \rho_q \tag{4}$$

and,

$$\rho_q = -\frac{\alpha}{2}\frac{3w_q}{r^{3(1+w_q)}} \tag{5}$$

p_q is the pressure and ρ_q is the energy density of the matter. To cause acceleration, the pressure p_q has to be negative, and the matter energy density ρ_q is positive. Since w_q is negative, to obtain a positive pressure, the parameter α has to be positive. The basis for the choices of the parameters and for details on the derivation of the metric, reader is referred to the original paper of Kiselev [9].

For $-1/3 \leq w_q < 1$, the solutions are asymptotically flat. For the range, $-1 < w_q < -1/3$, the space-time is non-asymptotically flat.

There are few works that have focused on studying this black hole. Thermodynamics and phase transitions has been studied in [11] for charged black holes for all

possible values of w_q. In [12], the authors studied the thermodynamics of only the asymptotically flat solutions and observed second order phase transitions. Quasinormal modes for a charged black hole surrounded by dark energy has been studied in [13]. The null geodesics of the neutral black hole surrounded by the quintessence has been studied by Fernando in [14]

When $w_q = -1$, the function $f(r)$ reduces to,

$$f(r) = 1 - \frac{2M}{r} + \frac{Q^2}{r^2} - \alpha r^2 \tag{6}$$

which is the Reissner–Nordstrom-de Sitter black hole (one can replace $\alpha = \frac{\Lambda}{3}$ where Λ is the cosmological constant).

In the rest of the paper, we will choose $w_q = -\frac{2}{3}$ as the simplest, nontrivial charged black hole surrounded by the quintessence to study. This assumption will lead to the metric in consideration to be,

$$ds^2 = -f(r)dt^2 + \frac{dr^2}{f(r)} + r^2(d\theta^2 + sin^2\theta d\phi^2) \tag{7}$$

with,

$$f(r) = 1 - \frac{2M}{r} + \frac{Q^2}{r^2} - \alpha r \tag{8}$$

Hence, the black hole discussed in this paper is non-asymptotically flat and has a curvature singularity at $r = 0$.

3 Free quintessence space-time with $M = 0$ and $Q = 0$

When the mass and charge are zero, the geometry of the metric in Eq. (7) simplifies to the free-quintessence space-time given by,

$$ds^2 = -(1 - \alpha r)dt^2 + \frac{dr^2}{(1 - \alpha r)} + r^2(d\theta^2 + sin^2\theta d\phi^2) \tag{9}$$

Such a space-time has an outer horizon at $r_c = \frac{1}{\alpha}$. The space-time has a curvature scalar $R = \frac{6\alpha}{r}$. Hence there is a singularity at $r = 0$. This space-time is very similar to the de Sitter space-time which has the metric,

$$ds^2 = -\left(1 - \frac{\Lambda r^2}{3}\right)dt^2 + \frac{dr^2}{\left(1 - \frac{\Lambda r^2}{3}\right)} + r^2(d\theta^2 + sin^2\theta d\phi^2) \tag{10}$$

with an outer horizon at $r_c = \sqrt{\frac{3}{\Lambda}}$, which is the cosmological horizon (Fig. 1).

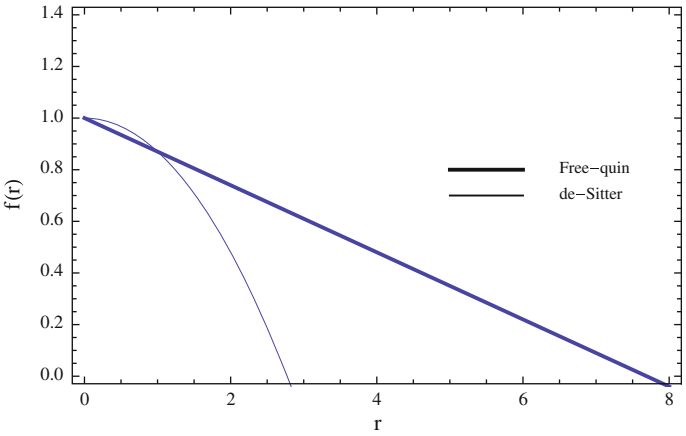

Fig. 1 The figure shows $f(r)$ versus r for free quintessence and the de Sitter space-time. Here $\alpha = \frac{\Lambda}{3} = 0.13$

The space-time with the free quintessence has the Hawking temperature,

$$T_{H(free\ quin)} = \frac{1}{4\pi}\left|\frac{dg_{tt}}{dr}\right|_{r=r_h} = \frac{\alpha}{4\pi} \tag{11}$$

The de Sitter cosmology has the background temperature as,

$$T_{H(de\ Sitter)} = \frac{1}{2\pi}\sqrt{\frac{\Lambda}{3}} \tag{12}$$

A detailed comparison of the free-quintessence space-time and the de Sitter space-time is presented in [9]. A description of the de-Sitter space-time can be found in the book by Griffiths and Podolsk$\acute{y}$ [10].

4 Reissner–Nordstrom black hole with and without the cosmological constant

In order to fully understand and appreciate the properties of the charged black holes with the quintessence, we will review properties of the Reissner–Nordstrom black hole and the Reissner–Nordstrom-de Sitter black hole in this section.

The Reissner–Nordstrom black hole is given by the metric,

$$f(r) = 1 - \frac{2M}{r} + \frac{Q^2}{r^2} \tag{13}$$

There are two horizons,

$$r_+ = M - \sqrt{M^2 - Q^2}; \quad r_{++} = M + \sqrt{M^2 - Q^2} \tag{14}$$

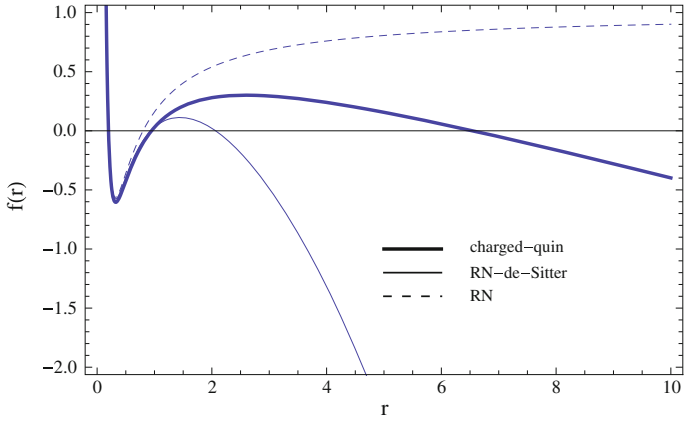

Fig. 2 The figure shows $f(r)$ versus r for charged black hole with the quintessence, Reissner–Nordstrom black hole and and the Reissner–Nordstrom-de Sitter space-time. Here $M = 0.5$, $Q = 0.4$ and $\alpha = \frac{\Lambda}{3} = 0.13$

Black hole exists only when $M \geq Q$. Hence the $Q_{critical} = M$. When $Q = Q_{critical}$, there is a degenerate horizon. When $Q < Q_{critical}$, there are two horizons. When $Q > Q_{critical}$, there are no horizons and the solution becomes a naked singularity (Fig. 2).

Since both the cosmological constant and the quintessence matter provide a mechanism for the acceleration of the universe, it is important to compare the charged black hole in de-Sitter space and with the quintessence matter. The Reissner–Nordstrom-de Sitter black hole has the metric,

$$ds^2 = -f(r)dt^2 + \frac{dr^2}{f(r)} + r^2(d\theta^2 + sin^2\theta d\phi^2) \tag{15}$$

with,

$$f(r) = 1 - \frac{2M}{r} + \frac{Q^2}{r^2} - \frac{\Lambda}{3}r^2 \tag{16}$$

Reissner–Nordstrom-de Sitter black hole also has the possibility of having three horizons for the appropriate values of M, Q and Λ: inner black hole horizon (r_+), outer black hole horizon(r_{++}) and the cosmological horizon (r_c). The quantum global structure of the de Sitter space and the charged black holes in de Sitter space is discussed in detail in [15]. The two horizons, r_{++} and r_c, are not in thermal equilibrium. However, there are two families of the Reissner–Nordstrom-de-Sitter black hole in which the temperatures at the event horizon and the cosmological horizon are the same: charged Nariai black hole and the lukewarm black hole. Charged Nariai black hole is a solution where the cosmological horizon and the black hole horizon coincides. Even though the horizons seem to coincide, the proper distance between them are non-zero. Also, the temperature is non-zero and both horizons have the same temperature. A detailed description of the thermodynamics of the Reissner–Nordstrom-de Sitter black hole is

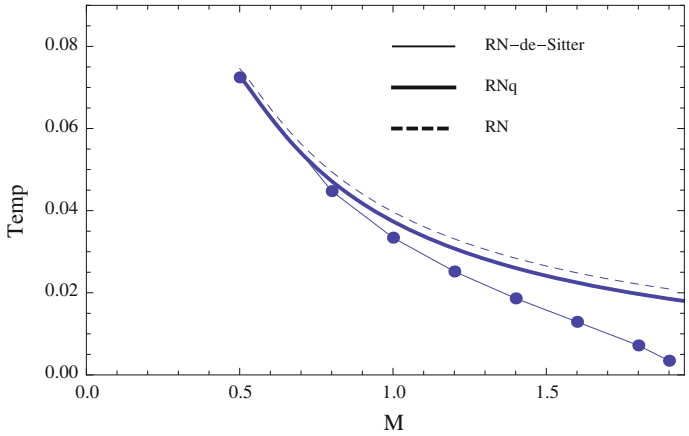

Fig. 3 The figure shows the graphs Temperature versus M for the charged black holes with the cosmological constant, without the cosmological constant, and with the quintessence matter. Here, $Q = 0.4$ and $\alpha = \frac{\Lambda}{3} = 0.01$

given in [16–18]. Instantons in the Reissner–Nordstrom-de Sitter space is discussed in [19,20]. Generalized Nariai solutions for Yang-type monopoles are discussed in [21]. Charged Nariai black hole with a dilaton is discussed in [22].

The temperature of the Reissner–Nordstrom-de-Sitter black hole is given by,

$$T_H = \frac{1}{4\pi r_{++}} \left| 1 - \frac{Q^2}{r_{++}^2} - 3\Lambda r_{++}^2 \right| \tag{17}$$

The temperature of a general charged black hole with the quintessence black hole is given by,

$$T_H = \frac{1}{4\pi r_{++}} \left| 1 - \frac{Q^2}{r_{++}^2} - 2\alpha r_{++} \right| \tag{18}$$

From the graph in Fig. 3, it is clear that Reissner–Nordstrom-de Sitter black hole is colder than the others.

5 The solution space for the horizons of the charged black hole with the quintessence

The horizons for the black holes are obtained from the roots of the function $f(r) = 0$ given by,

$$\alpha r^3 - r^2 + 2Mr - Q^2 = 0 \tag{19}$$

which is a cubic equation. We use well known results on the roots of a cubic polynomial here. The discriminant $\triangle$ for the cubic equation in Eq. (19) is given by,

$$\triangle = 4(M^2 - Q^2) + \alpha(-32M^3 + 36Q^2M) - 27\alpha^2Q^4 \tag{20}$$

Note that when $\alpha = 0$, the discriminant $\triangle = 4(M^2 - Q^2)$ which indicates the nature of the roots of the Reissner–Nordstrom black hole. Depending on the sign of $\triangle$, there would be one horizon(degenerate case), two horizons or no horizons.

Now getting back to the case for $\alpha \neq 0$, we will analyze all the possibilities in the following sections.

5.1 Structure of roots for fixed M

Now, one can study the behavior of $\triangle$ for fixed M and varying Q. One can solve $\triangle = 0$ for $Q_{critical}$ in terms of M and α. Since $\triangle$ is function of Q^2, it can be easily solved to be

$$Q^2_{critical(1,2)} = \frac{2\left(-1 + 9\alpha M \pm \sqrt{1 - 18\alpha M + 108\alpha^2M^2 - 216\alpha^3M^3}\right)}{27\alpha^2} \tag{21}$$

$Q^2_{critical(1,2)}$ is plotted in the Fig. 4. One can observe that $Q^2_{critical1} > 0$ for all values of M while $Q^2_{critical2} > 0$ only for range of values of M.

In Figs. 5 and 6, the $Q_{critical}$ is plotted with M. The function $f(r)$ is plotted for one particular value of M and the corresponding $Q_{critical}$. It is clear that the location of the degenerate root differs for $Q_{critical1}$ and $Q_{critical2}$.

Now that we have understood $\triangle = 0$ case well, one can study what type of roots are given for $f(r) = 0$ for non-zero values of $\triangle$. The graph Fig. 7 shows how $\triangle$ changes with Q and the corresponding possibilities for the roots of $f(r) = 0$. The

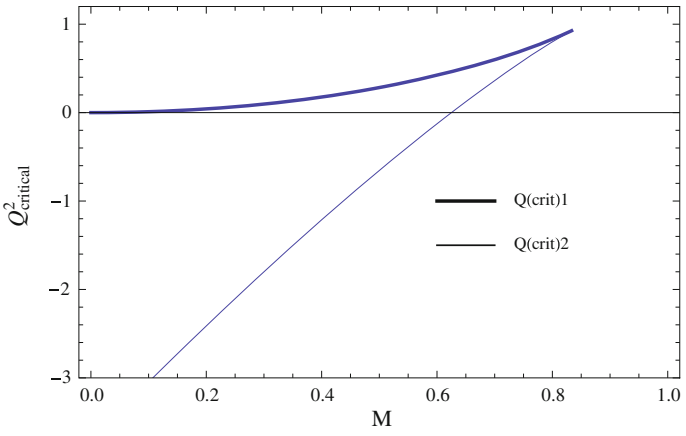

Fig. 4 The figure shows the graphs for $Q^2_{critical(1,2)}$ versus M. Here $\alpha = 0.2$

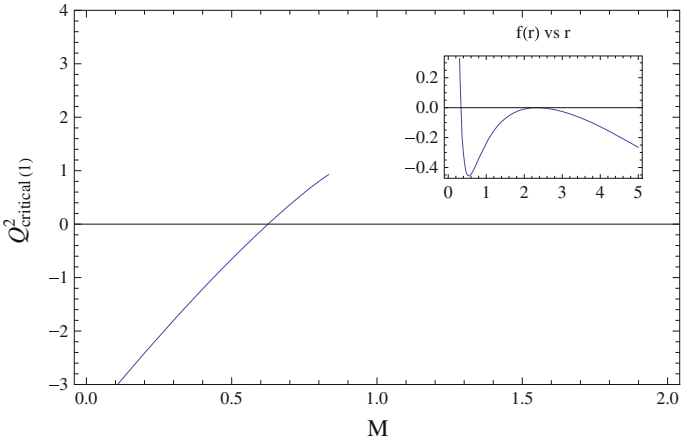

Fig. 5 The figure shows the $Q_{critical}1$ versus M. The function $f(r)$ is plotted for $M = 0.7$ and $Q_{critical1} = 0.6025$. Here $\alpha = 0.2$

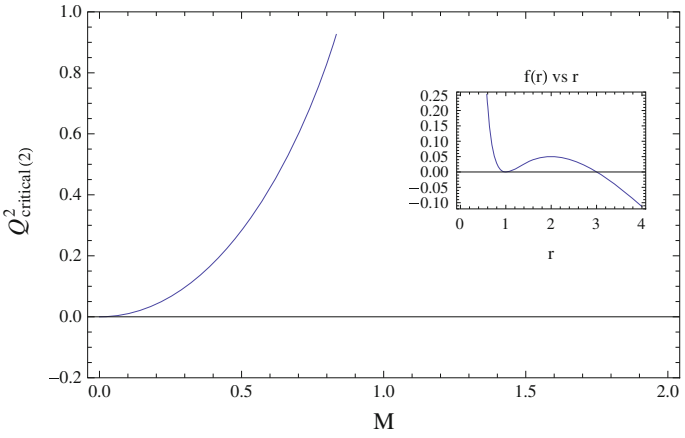

Fig. 6 The figure shows the $Q_{critical2}$ versus M. The function $f(r)$ is plotted for $M = 0.7$ and $Q_{critical2} = 0.7746$. Here $\alpha = 0.2$

corresponding behavior for $f(r)$ is also plotted underneath it. Each possibility gives different scenarios for the horizons.

In the Fig. 8, the function $f(r)$ is plotted for three values of Q with fixed M.

5.2 Structure of roots for fixed Q

Now, one can study the behavior of $\triangle$ for fixed Q and varying M. One can solve $\triangle = 0$ for $M_{critical}$ in terms of Q and α. Since $\triangle$ is a cubic polynomial in M, there will be three roots for $M_{critical}$ (given Q and α). The solution is quite lengthy and we will avoid writing the expressions explicitly. The three solutions for $M_{critical}$ are plotted in Fig. 9. The first and the second are realistic values since the other is negative.

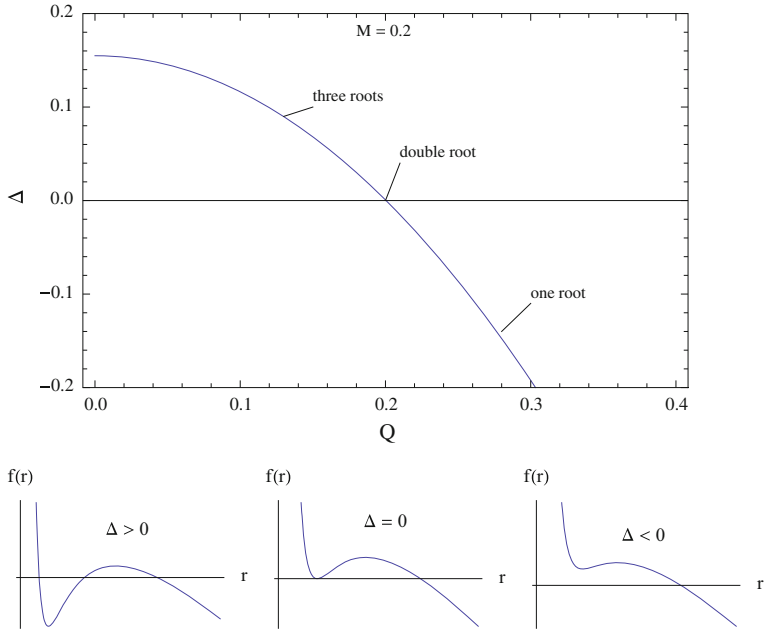

Fig. 7 The figure shows the $\triangle$ versus Q and the corresponding graphs $f(r)$ versus r. Here $Q = 1$ and $\alpha = 0.05$

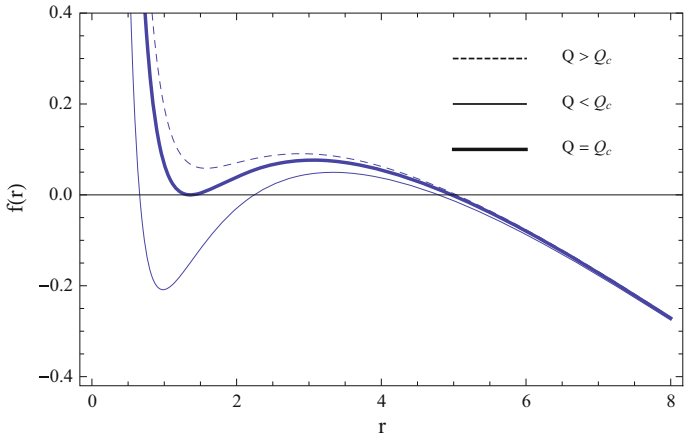

Fig. 8 The figure shows the $f(r)$ versus r for various values of Q

In Figs. 10 and 11, the $M_{critical}$ is plotted with Q. The function $f(r)$ is plotted for one particular value of Q and the corresponding $M_{critical}$, It is clear that the location of the degenerate root differs for $M_{critical1}$ and $M_{critical2}$.

Now that we have understood how $\triangle = 0$ case well, one can study what type of roots are given for $f(r) = 0$ for non-zero values of $\triangle$. The graph in Fig. 12 shows how $\triangle$ changes with M and the corresponding possibilities for the roots of $f(r) = 0$.

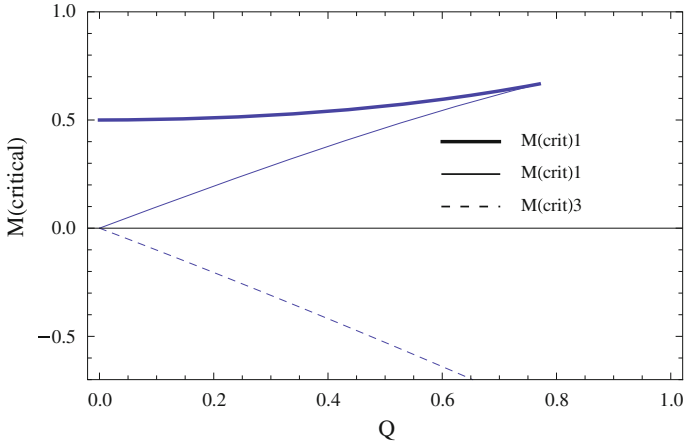

Fig. 9 The figure shows the $M_{critical}$ versus Q. The three roots are given in the three graphs. Here, $\alpha = 0.25$

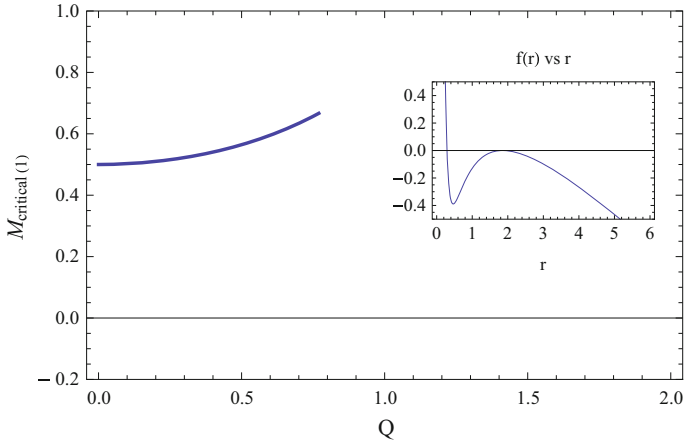

Fig. 10 The figure shows the $M_{critical}1$ versus Q. The function $f(r)$ is plotted for $Q = 0.5$ and $M_{critical1} = 0.5648$. Here $\alpha = 0.25$

The corresponding behavior for $f(r)$ is also plotted underneath it. Each possibility gives different scenarios for the horizons.

To summarize, for $M = M_{critical}$, there will be a degenerate horizon where two out of the three horizons will coincide. When $M > M_{critical}$, there will be only one horizon. When $M < M_{critical}$, there will be three horizons, the Cauchy horizon (r_+), the event horizon(r_{++}) and the cosmological horizon (r_c). This is represented for one particular case in Fig. 13.

5.3 Solution space

Summarizing all possibilities for horizons, one can draw the graph in Fig. 14 where M is plotted against Q. When $Q = 0$, one get free-quintessence, Neutral-quintessence

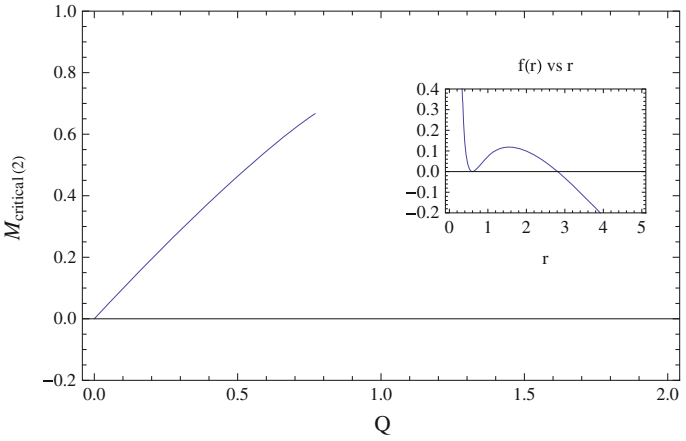

Fig. 11 The figure shows the $M_{critical2}$ versus Q. The function $f(r)$ is plotted for $Q = 0.5$ and $M_{critical2} = 0.4633$. Here $\alpha = 0.25$

and the Neutral–Nariai black hole. For other values of Q, when the points are inside the boundaries, one have the general charged-quintessence black hole with three horizons. On the boundaries, for $M = M_{critical1}$ one obtain charged Nariai black hole with the quintessence. The properties of such black holes will be described in detail in Sect. 7. When $M = M_{critical2}$, one obtain cold black holes with the quintessence. They are described in detail in Sect. 7. When both boundaries meet, one obtain the ultra cold black holes which have zero temperature. They are described in Sect. 8.

6 Number of horizons for the charged black hole with the quintessence

Depending on the values of M, Q and α, the function $f(r)$ could have one, two or three roots leading to different kind of black holes. Here, we will explicitly write down the horizon radius for all three different scenarios.

6.1 The black hole with three horizons

When $\triangle > 0$ there are three roots to the function $f(r)$. The smallest root corresponds to the black hole Cauchy horizon (r_+), the second one corresponds to the black hole event horizon (r_{++}) and the largest root corresponds to the cosmological horizon (r_c). Then, the three horizons are given by,

$$r_c = 2\sqrt{\frac{-p}{3}}cos\left(\frac{\theta}{3}\right) + \frac{1}{3\alpha} \tag{22}$$

$$r_{++} = 2\sqrt{\frac{-p}{3}}cos\left(\frac{\theta}{3} - \frac{2\pi}{3}\right) + \frac{1}{3\alpha} \tag{23}$$

$$r_+ = 2\sqrt{\frac{-p}{3}}cos\left(\frac{\theta}{3} - \frac{\pi}{3}\right) + \frac{1}{3\alpha} \tag{24}$$

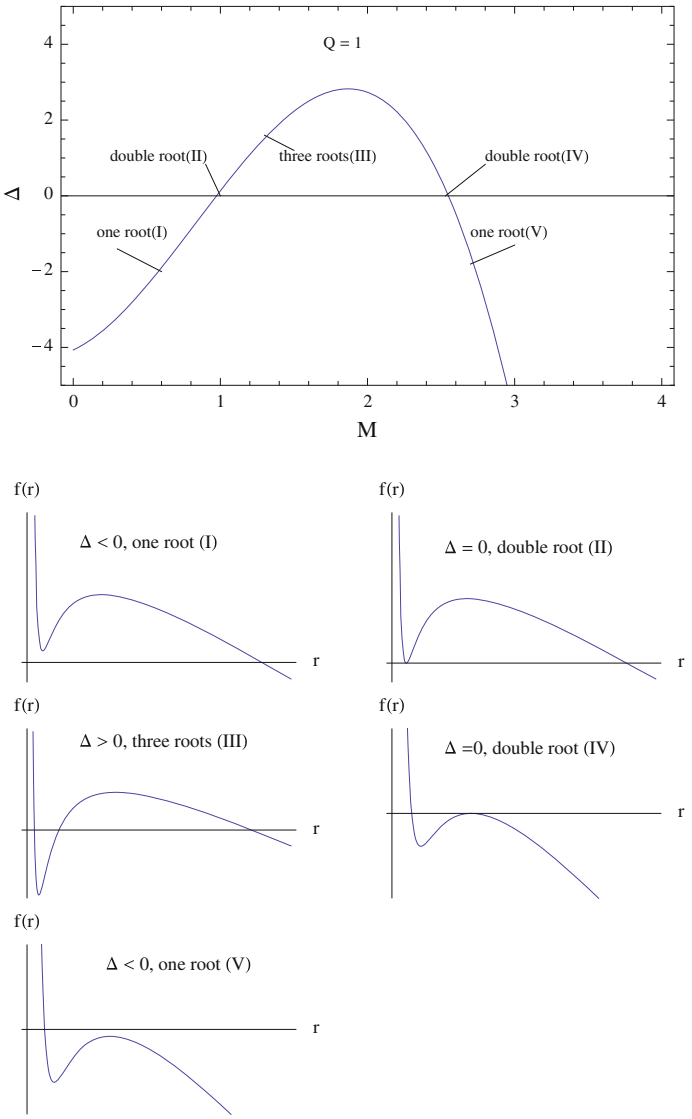

Fig. 12 The figure shows the $\triangle$ versus M and the corresponding graphs $f(r)$ versus r. Here $Q = 1$ and $\alpha = 0.05$

Here the three functions p, q and θ are,

$$p = \frac{(6M\alpha - 1)}{3\alpha^2} \tag{25}$$

$$q = \frac{(-2 + 18\alpha M - 27\alpha^2 Q^2)}{27\alpha^3} \tag{26}$$

$$\theta = cos^{-1}\left(\frac{3q}{2p}\sqrt{\frac{-3}{p}}\right) \tag{27}$$

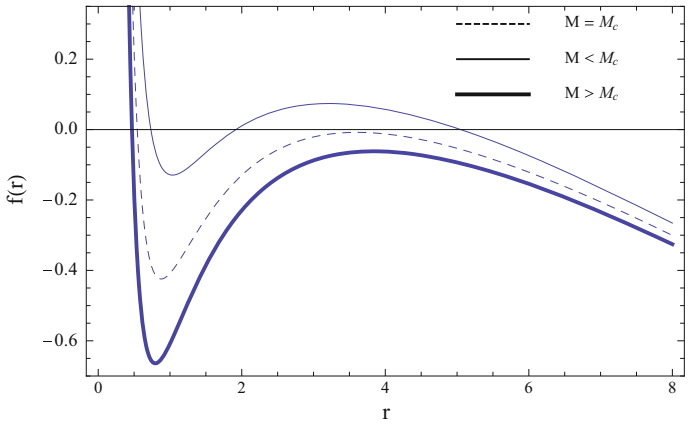

Fig. 13 The figure shows the graphs for $f(r)$ versus r for fixed charge and varying mass. Here $Q = 0.96$ and $\alpha = 0.13$

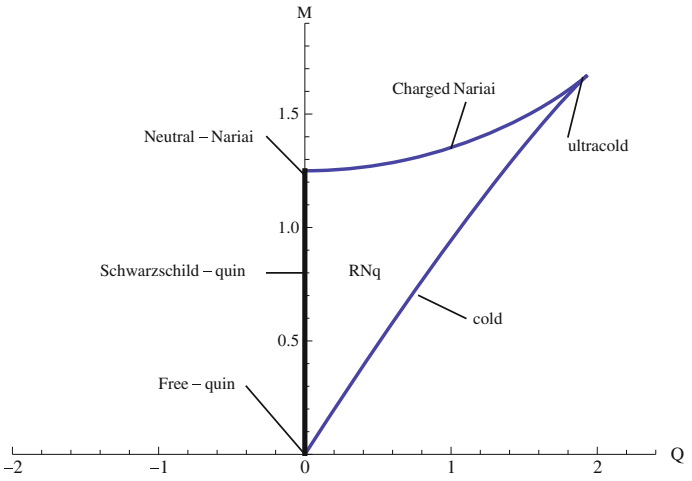

Fig. 14 The figure shows M versus Q graph. Here, $\alpha = 0.1$

Notice that for small α, the cosmological horizon $r_c \approx \frac{1}{\alpha}$ and $M \ll \frac{1}{\alpha}$. For the Reissner–Nordstrom-de-Sitter black hole, for special values of M, Q and the cosmological constant Λ, the possibility of three horizons exists [18]. The horizon at r_c here is similar to the cosmological horizon in the Reissner–Nordstrom-de-Sitter case.

6.2 Black hole with two horizons

In this case, there will be a double root and another simple root for the equation, $f(r) = 0$ as,

$$r_1 = r_2 = \frac{(9\alpha Q^2 - 2M)}{2(-1 + 6M\alpha)} \tag{28}$$

and,

$$r_3 = \frac{(-1 + 8\alpha M - 9\alpha^2 Q^2)}{\alpha(-1 + 6M\alpha)} \tag{29}$$

6.3 Black hole with one horizon

There are two possibilities to have only one horizon. One, is to have a triple root for $f(r) = 0$. The other is to have one real root and two complex conjugate roots for $f(r) = 0$.

6.3.1 Triple root

The triple real root given by,

$$r_1 = r_1 = r_3 = \frac{1}{3\alpha} \tag{30}$$

6.3.2 Black hole with one horizon and non zero temperature

In this case, there are two separate scenarios.

Case 1: $M < \frac{1}{6\alpha}, (p < 0)$

$$\eta = \frac{-q}{2}\left(\frac{3}{|p|}\right)^{(3/2)} \tag{31}$$

Here, the real root is given by,

$$x_{real} = \frac{|\eta|}{\eta}\sqrt{\frac{4|p|}{3}}cosh\left(\frac{1}{3}cosh^{-1}(|\eta|)\right) - \frac{1}{3\alpha} \tag{32}$$

Case 2: $M > \frac{1}{6\alpha}$ $(p > 0)$

Here, the real root is given by,

$$x_{real} = \sqrt{\frac{4|p|}{3}}sinh\left(\frac{1}{3}sinh^{-1}(|\eta|)\right) - \frac{1}{3\alpha} \tag{33}$$

Note that p and q are given by Eqs. (25) and (26).

7 Charged Nariai and cold black holes

According to the description in Sect. 5.2, when $\triangle = 0$ and $(-1 + 6M\alpha) \neq 0$, there are double roots and a simple root for the equation $f(r) = 0$. If the double roots occur at $r = \rho$, then,

$$f(\rho) = 0;\ f'(\rho) = 0 \tag{34}$$

By combining those two, one can obtain the following expressions for the charge Q and the mass M as,

$$M = \frac{\rho}{2}(2 - 3\alpha\rho) \tag{35}$$

$$Q^2 = \rho^2(1 - 2\alpha\rho) \tag{36}$$

By substituting the above value of M and Q and factorizing the function $f(r)$, it can be rewritten as,

$$f(r) = \frac{(r-\rho)^2\,(1 - \alpha(2\rho + r))}{r^2} \tag{37}$$

There is another positive real root b for the function $f(r)$ given by,

$$b = \frac{1}{\alpha} - 2\rho \tag{38}$$

which is derived from the function in Eq. (37). Now, one can write $f(r)$, M, Q, and α in terms of b and ρ as,

$$f(r)_{Nariai/cold}(r) = \frac{-(r-b)(r-\rho)^2}{r^2(b+2\rho)} \tag{39}$$

$$\alpha = \frac{1}{(b+2\rho)};\ M = \frac{\rho(2b+\rho)}{2(b+2\rho)};\ Q^2 = \frac{b\rho^2}{b+2\rho} \tag{40}$$

From the Sect. 5.2, the degenerate root ρ and the other simple root b can be written explicitly in terms of M and Q as,

$$\rho = \frac{-2M + 9\alpha Q^2)}{2(-1 + 6\alpha M)} \tag{41}$$

$$b = \frac{(-1 + 8\alpha M - 9\alpha^2 Q^2)}{\alpha(-1 + 6\alpha M)} \tag{42}$$

There are two possibilities for b: either it is outside the degenerate horizon ρ, or, it is inside the degenerate horizon. Which horizon is bigger depends on the expression,

$$\eta = -2 + 18\alpha M - 27\alpha^2 Q^2 \tag{43}$$

When $\eta < 0 \Rightarrow \rho < b$ and when $\eta > 0 \Rightarrow \rho > b$

The Hawking temperature at the horizon b is,

$$T_H(b) = \frac{(1 - \frac{\rho}{b})^2}{4\pi(b+2\rho)} \tag{44}$$

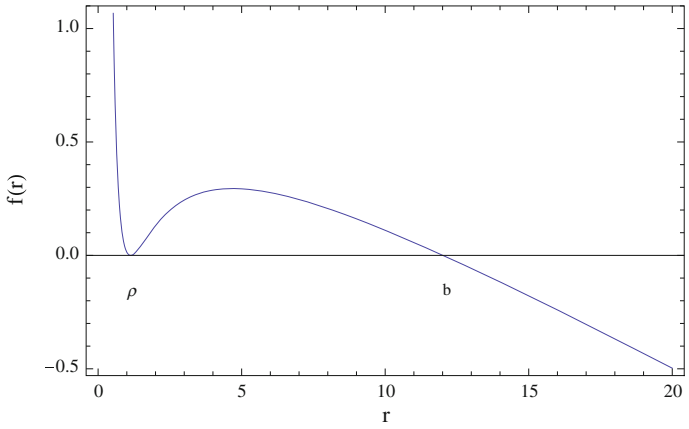

Fig. 15 The figure shows the graphs for $f(r)$ versus r for the cold black hole. Here $Q = 1.04121$, $M = 1$ and $\alpha = 0.07$

Since $\alpha = \frac{1}{b+2\rho}$,

$$T_H(b) = \frac{\alpha}{4\pi}\left(1 - \frac{\rho}{b}\right)^2 \tag{45}$$

Case 1 $(b > \rho)$**: Cold black hole**

When $b > \rho$, the black hole is called the cold black hole and,

$$b > \rho \Rightarrow 0 < \rho < \frac{1}{3\alpha} \tag{46}$$

Also, the temperature at the black hole event horizon, ρ is zero (Fig. 15).

If $b > \rho, \Rightarrow 1 - \frac{\rho}{b} < 1$ which leads to,

$$T_H(b) < \frac{\alpha}{4\pi} = T_H(free - quintessence) \tag{47}$$

Hence the temperature of the cosmological horizon is smaller due to the presence of the black hole compared to the free-quintessence case.

To understand the geometry near the degenerate horizon, we can choose a new coordinate y such as [23]

$$r = \rho - \epsilon y \tag{48}$$

The function $f(r)$ can be expanded around $r = \rho$ as,

$$f(r) \approx \frac{f''(\rho)}{2}(\epsilon y)^2 \tag{49}$$

Also, let a new time coordinate be defined as $\psi = \epsilon t$. With these transformations, the metric is approximated to be,

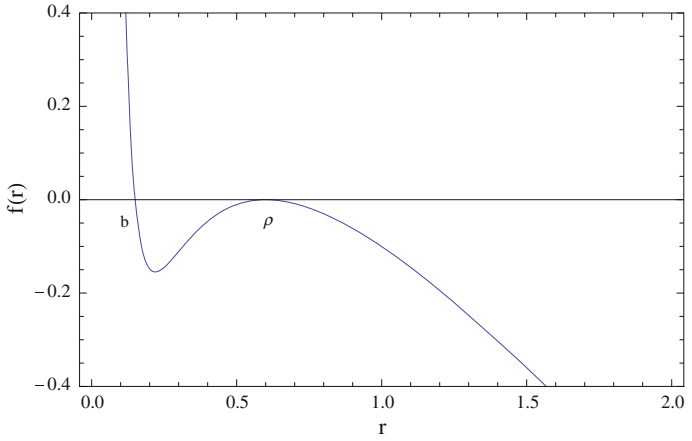

Fig. 16 The figure shows the graphs for $f(r)$ versus r for the charged Nariai black hole. Here $Q = 0.2$, $M = 0.2$ and $\alpha = 0.740741$

$$ds^2 = \frac{-f''(\rho)}{2} y^2 d\psi^2 + \frac{2}{f''(\rho)} \frac{dy^2}{y^2} + \rho^2 d\Omega^2 \tag{50}$$

Note that $f''(\rho) > 0$ for the cold black hole. The above geometry represents $AdS_2 \times S^2$ topology. The AdS_2 has the curvature $f''(\rho)/2$. The topology is the same for the cold Reissner–Nordstrom-de Sitter black hole but with curvature Λ (Fig. 15).

Case 2 ($b < \rho$)**: Charged Nariai black hole**

$$b < \rho \Rightarrow \frac{1}{3\alpha} < \rho < \frac{1}{2\alpha} \tag{51}$$

To find the geometry close to the degenerate horizon, one can approximate $f(r)$ (Fig. 16). by a parabola [10,24]

$$f(r) = \frac{f''(\rho)}{2}(r - r_1)(r - r_2) \tag{52}$$

Here, r_1 and r_2 represents a pair of close horizons, r_{++}, r_c. One can introduce new coordinates as,

$$t = \frac{2\psi}{\epsilon f''(\rho)}; \quad r = \rho + \epsilon cos\chi \tag{53}$$

$\chi = 0$ corresponds to r_1 and $\chi = \pi$ corresponds to r_2. Substituting these new coordinates to the metric will yield,

$$ds^2 = \frac{-2}{f''(\rho)} \left(-sin^2\chi d\psi^2 + d\chi^2\right) + \rho^2 d\Omega^2 \tag{54}$$

Note that $f''(\rho) < 0$ for the Nariai black hole. Now, the above geometry corresponds to $dS_2 \times S^2$. The curvature Λ_{eff} for dS_2 is given by $|f''(\rho)|/2$. Reissner–Nordstrom-de Sitter black hole also has the same topology near the degenerate horizon but with the curvature, Λ.

8 Ultra-cold black holes

A special case occurs when b and ρ coincides leading to a triple root for $f(r) = 0$. As discussed in Sect. (6.3.1), the triple real root is given by (Fig. 17),

$$r_+ = r_{++} = r_c = \frac{1}{3\alpha} \tag{55}$$

where,

$$M = \frac{1}{6\alpha}; \;\; Q = \frac{1}{3\sqrt{3}\alpha} \tag{56}$$

In this case,

$$f(\rho) = 0; \;\; f'(r)|_\rho = 0 \tag{57}$$

Hence the Hawking temperature, $T_H(\rho) = 0$.

To understand the geometry near the horizon, a new coordinate is defined as $y = \eta\sqrt{f''(\rho)/2}$. Since for the ultracold black hole $f''(\rho) = 0$, one can substitute the new coordinate and take the limit $f''(\rho) \to 0$ which leads to,

$$ds^2 = -\eta^2 d\psi^2 + d\eta^2 + \rho^2 d\Omega^2 \tag{58}$$

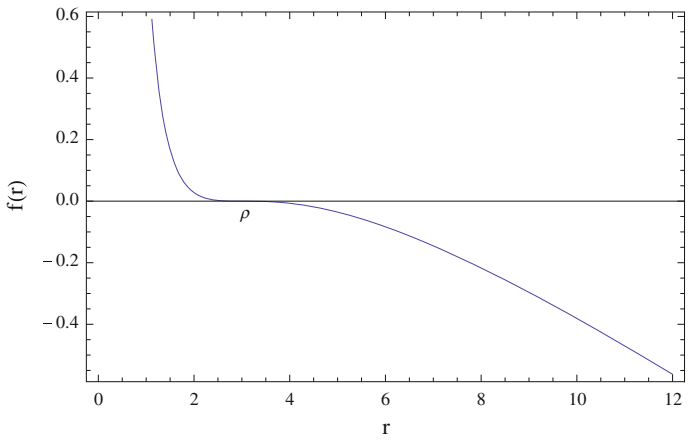

Fig. 17 The figure shows the graphs for $f(r)$ versus r for the ultracold black hole. Here $Q = 1.73205$, $M = 1.5$ and $\alpha = 0.1111$

The above geometry has the topology, $R^2 \times S^2$. This is similar to the topology of the ultracold Reissner–Nordstrom-de Sitter black hole near the degenerate horizon.

9 Lukewarm black holes with the quintessence

Lukewarm black hole is described as the charged-quintessence black hole solution describing a black hole with the same temperature at an outer horizon (or event horizon) a and the cosmological horizon b. Hence,

$$f(a) = f(b) = 0; \quad f'(a) = \pm f'(b) \tag{59}$$

The minus sign is chosen due to the nature of the graph at a and b. The Eq. (59) can be solved to obtain,

$$M = \frac{ab(a+b)}{a^2+3ab+b^2}; \quad Q^2 = \frac{a^2b^2}{a^2+3ab+b^2} \tag{60}$$

The function $f(r)$ can be re-written in terms of a and b as,

$$f(r) = \frac{\left(1-\frac{a}{r}\right)\left(1-\frac{b}{r}\right)(ab-(a+b)r)}{(a^2+3ab+b^2)} \tag{61}$$

The third root corresponding to the inner horizon of the black hole is at (Fig. 18),

$$r_+ = \frac{ab}{(a+b)} \tag{62}$$

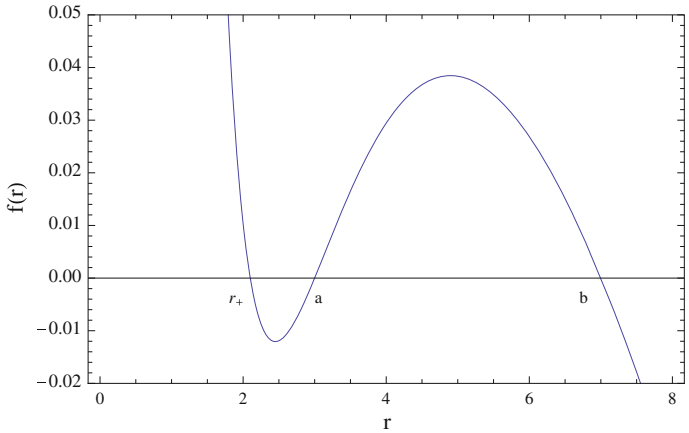

Fig. 18 The figure shows the graphs $f(r)$ versus r for the lukewarm Reissner–Nordstrom black hole surrounded by the quintessence. Here $a = 3$ and $b = 7$

Now, the temperature at a and b is,

$$T(a) = T(b) = \frac{1}{4\pi}|f'(a)| = \frac{1}{4\pi}\frac{|b-a|}{(a^2+3ab+b^2)} \tag{63}$$

Lukewarm black holes for the Reissner–Nordstrom black holes are discussed in [18]. Lukewarm black holes for the quadratic gravity is presented in [25].

10 Conclusions

We have investigated solution space for the charged black hole surrounded by the quintessence. The mass M and the charge Q are varied to obtain various configurations for the solutions for the horizon radii. Depending on the values of M, Q and α, it is possible to have three or two horizons or a single horizon.

When the horizons coincide, interesting class of black hole space-times emerges. When the Cauchy and the event horizons coincide, a cold black hole with a zero temperature emerges. The topology of this space time near the horizon is $AdS_2 \times S^2$. When the cosmological and the event horizon coincide, charged Nariai type black hole emerges. The topology at the near horizon is $dS_2 \times S^2$. An ultra-cold black hole is a result of all three horizons converging to one. Near the horizon, this black hole has the topology $R^2 \times S^2$. Another black hole named the lukewarm black hole emerge when the temperature of the event horizon and the cosmological horizon are the same. All these configurations are similar to what is studied in the Reissner–Nordstrom-de Sitter black hole.

One can also study the topology of the Nariai, cold and ultracold black holes with the quintessence with general w_q values (with $-1 < w_q < -1/3$). If degenerate horizons exists, they are at $\tilde{\rho} = \frac{Q^2(w_q-1)}{2Mw_q}$. The topology of the Nariai, cold and ultracold black holes will be the same as for the one with $w_q = -2/3$ but with curvature of dS_2 and AdS_2 given by $\pm|f''(\tilde{\rho})|/2$.

References

1. Perlmutter, S., et al.: Measurements of Ω and Λ from 42 high-redshift supernovae. Astrophys. J. **517**, 565 (1999)
2. Riess, A.G., et al.: Observational evidence from supernovae for an accelerating universe and a cosmological constant. Astron. J. **116**, 1009 (1998)
3. Riess, A.G., et al.: BVRI light curves for 22 Type Ia supernovae. Astron. J. **117**, 707 (1999)
4. Copeland, E.J., Sami, M., Tsujikawa, S.: Dynamics of dark energy. Int. J. Mod. Phys. D **15**, 1753 (2006)
5. Wang, P., Wu, P., Yu, H.: A new extended quintessence, arXiv:1301.5832
6. Avelino, P.P.: Quintessence and tachyon dark energy with a constant equation of state parameter. Phys. Lett. **B699**, 10 (2011)
7. Farooq, M.U., Jamil, M., Debnath, U.: Dynamics of interacting phantom and quintessence dark energy. Astrophys. Space Sci. **334**, 243 (2011)
8. Romalis, M.V., Caldwell, R.R.: Laboratory search for a quintessence field. arXiv:1302.1579
9. Kiselev, V.V.: Quintessence and black holes. Class. Quantum Grav. **20**, 1187 (2003)
10. Griffiths, J.B., Podolský, J.: Exact space-times in Einstein general relativity (Cambridge Monographs on Mathematical Physics). Cambridge University Press, Cambridge (2009)

11. Thomas, B.B., Saleh, M., Kofane, T.C.: Thermodynamics and phase transition of the Reissner-Nordstrom black hole surrounded by quintessence. Gen. Relativ. Gravit. **44**, 2181 (2012)
12. Azreg-Ainou, M., Rodrigues, M.E.: Thermodynamical, geometrical and Poincare methods for charged black holes in presence of quintessence. arXiv:1211.5909
13. Varghesee, N., Kuriakose, V.C.: Quasinormal modes of Reisnner-Nordstrom black hole surrounded by quiontessence. Gen. Relativ. Gravit. **41**, 1249 (2009)
14. Fernando, S.: Schwarzschild black hole surrounded by quintessence: null geodesics. Gen. Relativ. Gravit. **44**, 1857 (2012)
15. Bousso, R.: Quantum global structure of de Sitter space. Phys. Rev. **D60**, 063503 (1999)
16. Astefanesei, D., Mann, R.B., Radu, E.: Reissner-Nordstrom-de Sitter black hole, planar coordinates and dS/CFT. JHEP **029**, 0401 (2004)
17. Belgiorno, F., Caciatori, S.L., Piazza, F.D.: Pair-production of charged Dirac particles on charged Nariai and ultracold black hole manifolds. JHEP **028**, 0908 (2009)
18. Romans, I.J.: Supersymmetric, cold and lukewarm black holes in cosmological Einstein-Maxwell theory. Nucl. Phys. **B383**, 395 (1992)
19. Hawking, S.W., Ross, S.F.: Duality between electric and magnetic black holes. Phys. Rev. D **52**, 5865 (1995)
20. Mann, R.B., Ross, S.F.: Cosmological production of charged black hole pairs. Phys. Rev. D **52**, 2254 (1995)
21. Diaz, P., Segui, A.: Generalized Nariai solutions for Yang-type monopoles. Phys. Rev. D **76**, 064033 (2007)
22. Bousso, R.: Charged Nariai black hole with a dilaton. Phys. Rev. D **55**, 3614 (1999)
23. Cho, J., Nam, S.: Non-supersymmetric attractor with the Cosmological constant. JHEP **0707**, 011 (2007)
24. Matyjasek, J., Sadurski, P., Tryniecki, D.: Inside the degenerate horizons of the regular black holes. arXiv:1304.6347
25. Matyjasek, J., Zwierzchowska, K.: Lukewarm black holes in quadratic gravity. Mod. Phys. Lett. **A26**, 999 (2011)